

Global Aurora on Mars during the September 2017 Space Weather Event

Nicholas M. Schneider, Sonal K. Jain, Justin Deighan, Nasr Camella-Rosa, David A. Brain, Davin Larson, Robert J. Lillis, Ali Rahmati, Jasper S Halekas, Christina O. Lee, et al.

▶ **To cite this version:**

Nicholas M. Schneider, Sonal K. Jain, Justin Deighan, Nasr Camella-Rosa, David A. Brain, et al.. Global Aurora on Mars during the September 2017 Space Weather Event. Geophysical Research Letters, 2018, 45 (15), pp.7391-7398. 10.1029/2018GL077772 . insu-01803835

HAL Id: insu-01803835
https://insu.hal.science/insu-01803835

Submitted on 6 Aug 2020

HAL is a multi-disciplinary open access archive for the deposit and dissemination of scientific research documents, whether they are published or not. The documents may come from teaching and research institutions in France or abroad, or from public or private research centers.

L'archive ouverte pluridisciplinaire **HAL**, est destinée au dépôt et à la diffusion de documents scientifiques de niveau recherche, publiés ou non, émanant des établissements d'enseignement et de recherche français ou étrangers, des laboratoires publics ou privés.

AGU100 ADVANCING EARTH AND SPACE SCIENCE

Geophysical Research Letters

RESEARCH LETTER
10.1029/2018GL077772

Special Section:
Impact of the Sept. 10, 2017, solar event on Mars

Global Aurora on Mars During the September 2017 Space Weather Event

N. M. Schneider[1], S. K. Jain[1], J. Deighan[1], C. R. Nasr[1], D. A. Brain[1], D. Larson[2], R. Lillis[2], Ali Rahmati[2], J. S. Halekas[3], C. O. Lee[2], M. S. Chaffin[1], A. Stiepen[4], M. Crismani[1], J. S. Evans[5], M. H. Stevens[6], D. Y. Lo[7], W. E. McClintock[1], A. I. F. Stewart[1], R. V. Yelle[7], J. T. Clarke[8], G. M. Holsclaw[1], F. Lefevre[9], F. Montmessin[9], and B. M. Jakosky[1]

[1]Laboratory for Atmospheric and Space Physics, University of Colorado at Boulder, Boulder, CO, USA, [2]Space Science Laboratory, University of California, Berkeley, CA, USA, [3]Department of Physics and Astronomy, University of Iowa, Iowa City, IA, USA, [4]Laboratory for Planetary and Atmospheric Physics, Université de Liège, Liège, Belgium, [5]Computational Physics, Inc., Springfield, VA, USA, [6]Space Science Division, Naval Research Laboratory, Washington, DC, USA, [7]Lunar and Planetary Lab, University of Arizona, Tucson, AZ, USA, [8]Center for Space Physics, Boston University, Boston, MA, USA, [9]LATMOS/IPSL, Guyancourt, France

Key Points:
- The MAVEN spacecraft has obtained the first images of aurora on Mars
- Mars aurora can be global in nature, due to its lack of a global magnetic field
- The global aurora was triggered by a space weather event observed by many instruments and spacecraft

Correspondence to:
N. M. Schneider,
nick.schneider@lasp.colorado.edu

Citation:
Schneider, N. M., Jain, S. K., Deighan, J., Nasr, C. R., Brain, D. A., Larson, D., et al. (2018). Global aurora on Mars during the September 2017 space weather event. *Geophysical Research Letters*, *45*, 7391–7398. https://doi.org/10.1029/2018GL077772

Received 14 MAR 2018
Accepted 21 MAY 2018
Accepted article online 29 MAY 2018
Published online 4 AUG 2018

©2018. American Geophysical Union. All Rights Reserved.

Abstract We report the detection of bright aurora spanning Mars' nightside during the space weather event occurring in September 2017. The phenomenon was similar to diffuse aurora detected previously at Mars, but 25 times brighter and detectable over the entire visible nightside. The observations were made with the Imaging UltraViolet Spectrograph, a remote sensing instrument on the Mars Atmosphere and Volatile EvolutioN spacecraft orbiting Mars. Images show that the emission was brightest around the limb of the planet, with a fairly uniform faint glow against the disk itself. Spectra identified four molecular emissions associated with aurora, and limb scans show the emission originated from an altitude of ~60 km in the atmosphere. Both are consistent with very high energy particle precipitation. The auroral brightening peaked around 13 September, when the flux of solar energetic electrons and protons both peaked. During the declining phase of the event, faint but statistically significant auroral emissions briefly appeared against the disk of the planet in the form of narrow wisps and small patches. These features are approximately aligned with predicted open field lines in the region of strong crustal magnetic fields in Mars' southern hemisphere.

Plain Language Summary A solar storm caused energetic particles from the Sun to strike Mars atmosphere and cause aurora. Unlike Earth, where aurora are limited to polar regions at the edges of our magnetic field, Mars aurora engulfed the entire planet. This is due to Mars' lack of a strong, global magnetic field. The solar storm caused aurora 25 times brighter than any previously observed. Mars Atmosphere and Volatile EvolutioN's Imaging UltraViolet Spectrograph obtained the first images of aurora on Mars. Mars does have weak magnetic fields locked into its wrist in some places. Imaging UltraViolet Spectrograph also obtained the first images of patchy aurora in those regions.

1. Introduction

The Mars Atmosphere and Volatile EvolutioN (MAVEN) spacecraft has been orbiting Mars since 21 September 2014, with a primary mission to study the behavior of the upper atmosphere and the escape of its constituent gases to space (Jakosky et al., 2014). MAVEN orbits Mars on a 4.5-hr elliptical orbit, with a closest approach to Mars' surface at periapse of 150–200 km and an apoapse around 5,900 km at the time of the observations. MAVEN carries one remote sensing instrument for the study of Mars' upper atmosphere, the Imaging UltraViolet Spectrograph (IUVS; McClintock et al., 2015). The instrument captures spectra of the planet and its atmosphere in the far-UV (110–190 nm) and middle UV (180–340 nm), ideal for recording well-known atmospheric emissions from CO_2 and its dissociation and ionization products. The instrument is mounted on an articulated payload platform that can orient IUVS's field of view relative to Mars depending on spacecraft location, orientation, and desired viewing geometry. IUVS was designed to observe Mars dayglow, nightglow, hydrogen corona, *D*/*H* ratio, and stellar occultations and is also sensitive to auroral emissions.

Mars exhibits at least three types of aurora. The SPICAM instrument on Mars Express discovered discrete aurora: small short-lived patches of aurora related to the crustal magnetic fields in Mars' southern hemisphere

(Bertaux et al., 2005). Discrete aurora have been attributed to particles accelerated to energies <1 keV by magnetic field reconfiguration at Mars and have been primarily observed at altitudes around 140 km (Brain et al., 2006; Gérard et al., 2015).

Mars Atmosphere and Volatile EvolutioN/IUVS discovered a second type called diffuse aurora (Schneider, Deighan, Jain, et al., 2015), with emissions spanning much of Mars' nightside for 5 days in December 2014. The phenomenon was observed again in March 2015 (Jakosky et al., 2015) and has been seen occasionally since. Diffuse aurora are attributed to solar energetic particles (SEPs), specifically electrons accelerated to energies of ~100 keV at the Sun and heliospheric shock fronts. MAVEN carries an instrument also abbreviated SEP dedicated to the detection of such particles (Larson et al., 2015); hereafter, we refer to it as MAVEN/SEP. Such particles can penetrate to great depths in the atmosphere, and IUVS observations yielded peak emissions altitudes in the range 60–70 km. Theoretical work by Gerard et al. (2017) confirmed that 100-keV electrons are capable of exciting auroral emission at 60 km altitude, but neither that work nor Schneider, Deighan, Jain, et al. (2015) was able to demonstrate that the observed emission profile could be modeled quantitatively by emission from the precipitating electron population.

Mars Atmosphere and Volatile EvolutioN/IUVS also discovered a third form called proton aurora occurring on Mars' dayside, caused by penetrating protons from the solar wind (Deighan et al., 2018; Halekas, 2017). The MAVEN/IUVS detection of proton aurora prompted a search in the Mars Express SPICAM archive (Ritter et al., 2018), finding six events and confirming the existence of the phenomenon.

2. Observations

Two of IUVS's observing modes captured aurora emissions. As neither of these modes have been employed in previously published studies, we briefly describe them below.

First, IUVS obtains ultraviolet spectral images of Mars' disk during the 70 min surrounding apoapse. Since the spectrograph uses an entrance slit, the slit must be scanned across Mars' ~55° diameter disk to construct an image. Since the IUVS slit spans 11°, only a narrow swath across the planet can be recorded at a time. The complete image can be constructed by taking advantage of spacecraft motion about the planet, allowing several image swaths to be taken sequentially while the spacecraft is inertially pointed. Note that the ~70-min duration of imaging and the changing viewing geometry means that the image should not be considered a snapshot from a single location at a moment in time. Slit pointings on and near Mars' dayside use low intensifier gain to avoid saturating the detector. Nightside pointings use high gain for optimum sensitivity to faint emissions. At each slit pointing, a spatially resolved spectrum is taken. The detector readout is binned spatially and spectrally according to the observation's scientific goals and the limits imposed by data downlink to Earth. For these observations, a limited middle UV spectral range 195–220 nm was recorded in 40 spectral bins, sufficient to capture and spectrally distinguish two important molecular emissions observed on Mars' nightside: CO Cameron bands observed in aurora and nitric oxide (NO) nightglow emissions. The spectra are fitted against templates for these two emissions using multiple linear regression (Stevens et al., 2015). Observations are normally taken every orbit, at 4.5-hr intervals, with occasional interruptions for data downlinks to Earth. The observation files used in this work are identified as "apoapse," version 12, of the Level 1b data available on the Planetary Data System (PDS).

Second, an alternative type of limb scans was used to provide complete spectra and vertical profiles of atmospheric emissions. Previous IUVS publications (e.g., Schneider, Deighan, Stewart, et al., 2015) used limb scans obtained during MAVEN's periapse. In September 2017, MAVEN's periapse lay on Mars' dayside such that these commonly used limb scans could not view Mars' nightside. IUVS also obtains limb scans during the orbit side segments as the spacecraft recedes from periapse and later approaches for the next periapse. The limb tangent point in this geometry lies approximately antipodal to periapse, hence lies on Mars nightside during this period. For side segment limb scans, the IUVS slit is pointed inward toward the orbit's line of apsides and oriented tangent to the limb. Spacecraft motion carries the inertially pointed slit upward or downward across the atmosphere at the limb. Small scan mirror repointings allow multiple limb scans to be obtained during each orbit side segment. For these observations, full spectral coverage can be recorded. This adds three nightside emissions to the CO Cameron band and NO emission recorded in imaging mode: the CO_2^+ ultraviolet doublet at 289 nm, the atomic oxygen line at 297.2 nm, and the CO_2^+ Fox-Duffendack-Barker bands between 300 and 340 nm. The observation files used in this work are identified as "inlimb" and

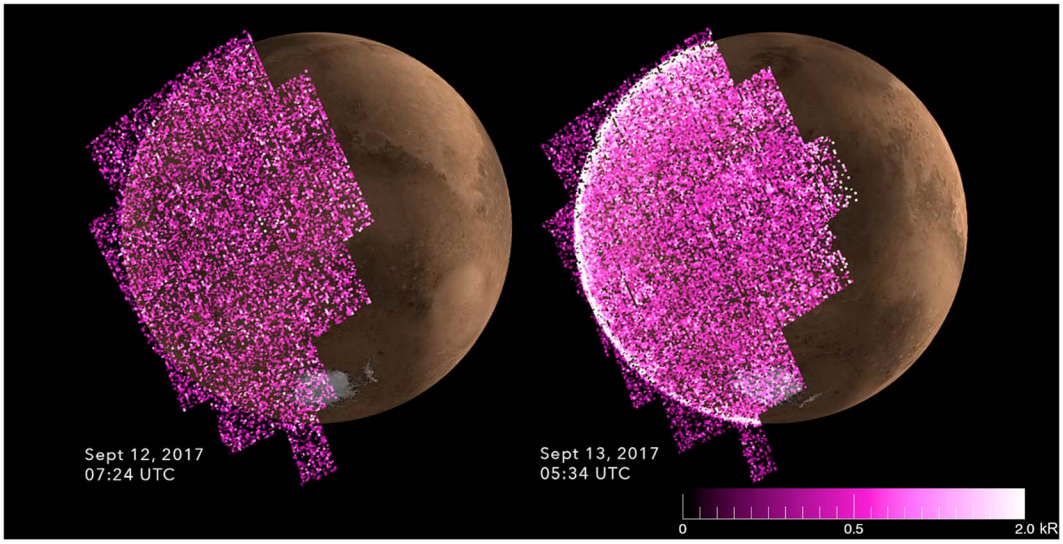


Figure 1. Midultraviolet images of Mars at the (left) start and (right) peak of the September 2017 space weather event. The purple-to-white brightness scale displays the brightness of emission matching the template for CO Cameron bands excited by particle precipitation, spanning the range 0–2.0 kR. The images were obtained on orbits 5726 and 5731 during Mars Atmosphere and Volatile EvolutioN's apoapse orbit segments. Imaging UltraViolet Spectrograph scanned its slit across Mars in six swaths from left to right, while the spacecraft traveled around Mars from top to bottom. In the right image, emission is enhanced across the entire disk, and especially around the limb where projection effects amplify the brightness. In the left image, the limb enhancement is barely visible, and the brightness of the disk is consistent with instrument noise and background. Auroral images were mapped onto the geographic coordinate system of the observation midpoint. Underlying the auroral images are simulated Mars views for the midpoints of the observations, with north up. The day/night terminator is evident across the right side, and the south polar cap at the bottom. Auroral detections were not possible on or near the illuminated crescent.

"outlimb," version 12, of the Level 1b data available at the PDS. Inlimb/outlimb pairs were obtained every four orbits due to timesharing with other observations.

3. Results

Figure 1 shows Mars nightside images taken at the start and at the peak of the space weather event, with brightness corresponding to the fitted spectrum of Cameron band emission as previously observed in Mars aurora. In the left image, Mars' disk shows a uniform background consistent with instrument noise, and the limb shows a faint but significant brightening. In the right image taken at the peak, all parts of the nightside observed at high gain show elevated emission; that is, aurora covers the entire observable nightside, and limb brightening of the optically thin emission is very pronounced. Auroral brightenings were observed in a total of 15 images over the 7–26 September period. Diffuse aurora, widespread across the nightside, had previously been detected in limb scan observations (Schneider, Deighan, Jain, et al., 2015), but the observations reported here are the first images of aurora of any type on Mars.

Figure 2 shows the spectrum and altitude profiles of the emission obtained from inlimb observations obtained during Orbit 5730 near the peak of the space weather event. The prominence of the CO_2^+ ultraviolet doublet emission compared to CO Cameron band emission is consistent with high-energy excitation associated with SEPs and diffuse aurora (Gérard et al., 2017), unlike the discrete aurora emissions dominated by CO Cameron bands. Both the spectrum and vertical profiles of Figure 2 are consistent with those reported in the discovery of diffuse aurora (Schneider, Deighan, Jain, et al., 2015, Jakosky et al., 2015) but at a brightness about 25 times higher in September 2017 than March 2015. Significant diffuse auroral emission was detected in an additional 20 inlimb or outlimb observations over the 7–26 September period. Periapse limb scan observations of Mars' dayside were optimal for the detection of proton aurora through H Lyman alpha emission, but no occurrences were detected.

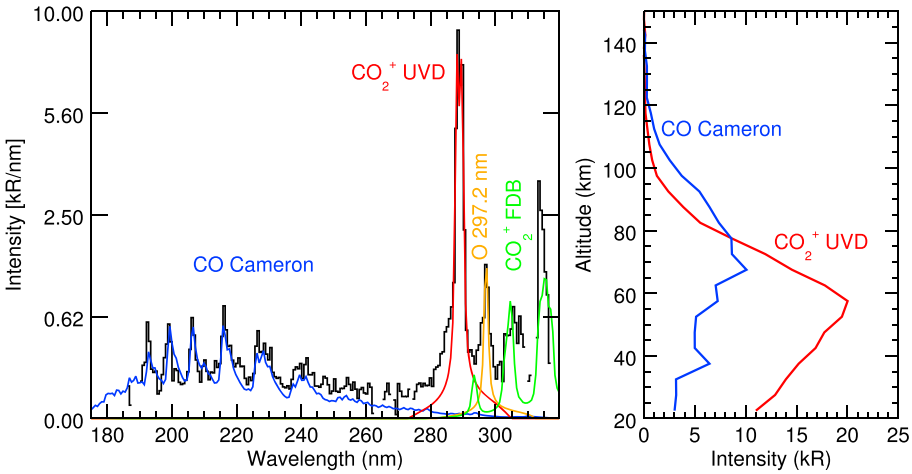


Figure 2. (left) Limb scan spectrum of the brightest auroral emission during orbit 5730, peaking at 60 km altitude. The data are shown in black, with templates for known molecular emissions scaled to match. The plot uses square root scaling to show detail in fainter emissions. (right) Vertical profiles of auroral emissions obtained from the same data, plotting the integrated intensity of the brightest two emissions versus altitude. The ultraviolet doublet (UVD) shows a sharp peak at 60 km altitude, while the CO Cameron bands show a broader peak around 70 km. The UVD profile primarily reveals the profile of molecular excitation through particle precipitation. In contrast, the Cameron band profile is strongly affected at low altitudes by deexcitation through collisional quenching. Note that dayglow, driven by the absorption of solar extreme ultraviolet radiation, occurs much higher at altitudes around 130 km.

Figure 3 shows the timeline of diffuse auroral detections and precipitating particle populations. The aurora exhibit three distinct events: 11–14 September, 17–18 September, and 20–21 September. The first is more than 10 times brighter than the other two. The primary auroral brightening during the first event correlates well with either MAVEN/SEP electrons or protons. The third auroral event corresponds better with MAVEN/SEP protons, but the second event has no corresponding rise in either MAVEN/SEP electrons or protons. It bears noting that MAVEN/SEP measurements are made thousands of kilometers away from the aurora themselves, so a perfect correlation is not expected. We conclude that comparison of the timelines alone does not identify a unique correlation with either MAVEN/SEP electrons or protons.

Figure 4 (top) shows an unusual phenomenon which only occurred on Orbit 5738 within this extended period. The approximately hour-long observation was obtained on 14 September 2018 centered around 12:46 UTC. Wisps and patches of potential auroral emission appeared across the nightside, unlike the bright limb glow and uniform disk emission of the other 15 apoapse images. Groups of pixels with enhanced brightness were identified by eye and given alphabetical identifiers. While the spectra associated with individual pixels have marginal signal-to-noise ratios, groups of such pixels can be coadded to compare their spectra to spectral templates for CO Cameron band emission, NO nightglow, or broadband features associated with cosmic rays or stray light occurring within the instrument. Wisps and patches whose spectra showed a good statistical match to Cameron band emission were color-coded purple, and those with poor statistics or spectral evidence of instrumental artifacts were coded orange. Note in particular that all of the horizontal linear features (E, F, G, J, and O) proved to be instrument artifacts. This is likely due to occasional cosmic rays, which affect a single slit position and detector readout which appears exactly horizontal in this coordinate system. The rest of the features are all consistent with auroral emission matching Cameron band emission.

We compared the locations of the auroral emissions with a statistical model of the Mars crustal magnetic field topology appropriate for the locations of the observations (Figure 4, bottom). We used the map from Brain et al. (2007) that shows the probability of open and closed magnetic field lines, based on Mars Global Surveyor measurements of electron pitch angle distributions at 400 km altitude. (Whether or not a particular geographic location is associated with an open or closed field line at any time or altitude depends on many factors, especially solar wind properties and Mars' orientation relative to the Mars-Sun line.) We transform the magnetic field map into the observational coordinate system, with the magnetic field topology pulled from the geographic footprint of each slit pointing at the instant of observation, allowing for slit motion, Mars'

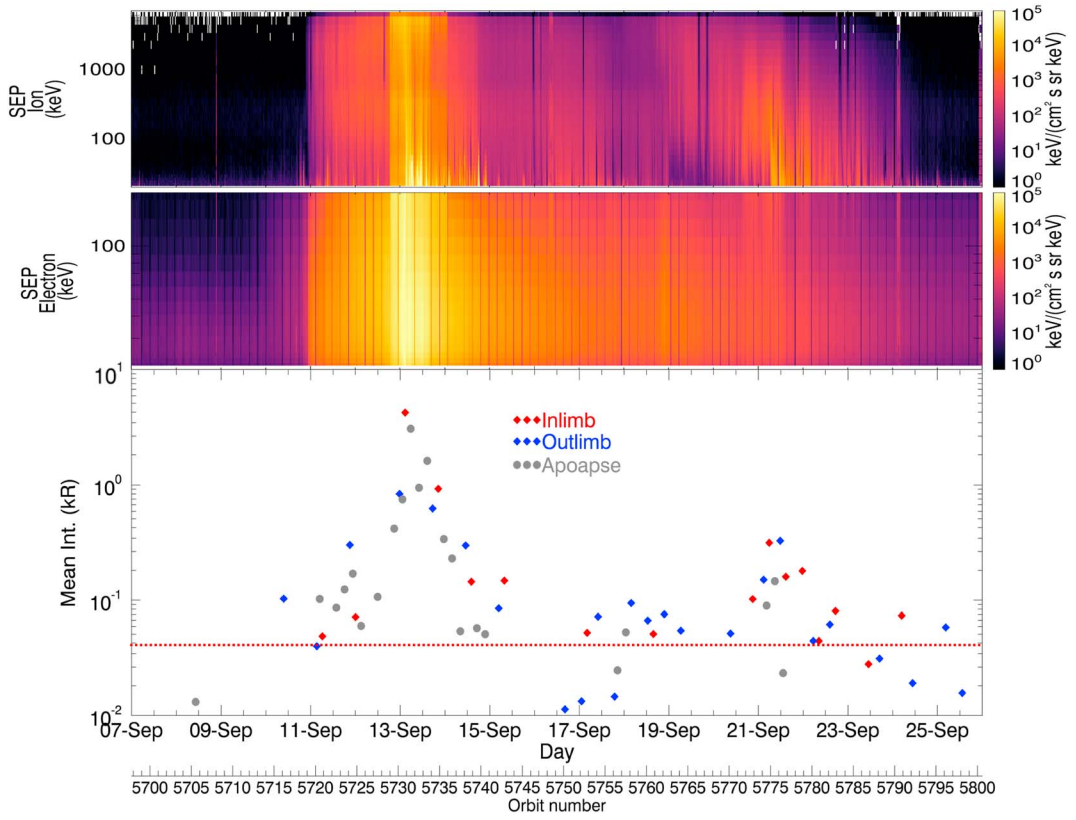


Figure 3. Timeline for auroral emissions and Mars Atmosphere and Volatile EvolutioN (MAVEN)/solar energetic particle (SEP) fluxes. The bottom panel shows auroral emission from CO Cameron bands in kiloRayleighs. The gray circles show brightnesses in the limb region averaged over 50–100 km extracted from apoapse images as in Figure 1. The red and blue diamonds show the brightness average of the same altitude range in limb scans across the emitting layer obtained about an hour before and after the apoapse images. Limb scans sampled the region roughly at the center of the disk seen in the apoapse images. The red line shows the instrument noise floor which sets a minimum detectable brightness of about 50 R. The timeline shows three auroral episodes, with the brightest one around 13 September at least 10 times brighter than the others. The top panels show MAVEN/SEP data, taken from Lee et al. (this issue), which are discussed in the text.

rotation, and spacecraft motion. We neglect the ~15 km (subpixel) maximum error between the planetodetic coordinate system of the observations and the planetocentric coordinate system of the topology map.

Figure 4 shows that all aurora emissions lie in or near regions with high probabilities of open field lines. Auroral emissions B, C, D, H, I, and L appear against Mars' disk on dark regions of the map. Auroral emissions A and P not only lie in regions of open crustal fields but also lie so close to the limb that their brightness could be attributed to limb enhancement instead. We count these two as inconclusive. Emissions K and M lie very close to statistically open field line regions, and further analysis may show them to be open under the exact magnetic field configuration, altitude, and solar wind at the time of the observations. All in all, the geographic locations of the observed features are consistent with the criteria for discrete aurora as originally observed by Mars Express/SPICAM.

The detection of discrete auroral emission features linked to crustal fields on Orbit 5738 is not an accident of favorable observing geometry. Several images with aurora visible at the limb offered favorable viewing of crustal magnetic fields but presented no statistically significant emission features that might be correlated with regions of open field lines. There is also no indication in the MAVEN/SEP data of changes in the precipitating particles over their entire energy ranges during this orbit. Although there is no specific trigger for so many discrete auroral emission features to occur on this orbit, the occurrence during the event's declining phase is consistent with the correlation pointed by out Brain et al. (2006) that local conditions for discrete aurora occur most often when the plasma environment as a whole is already disturbed.

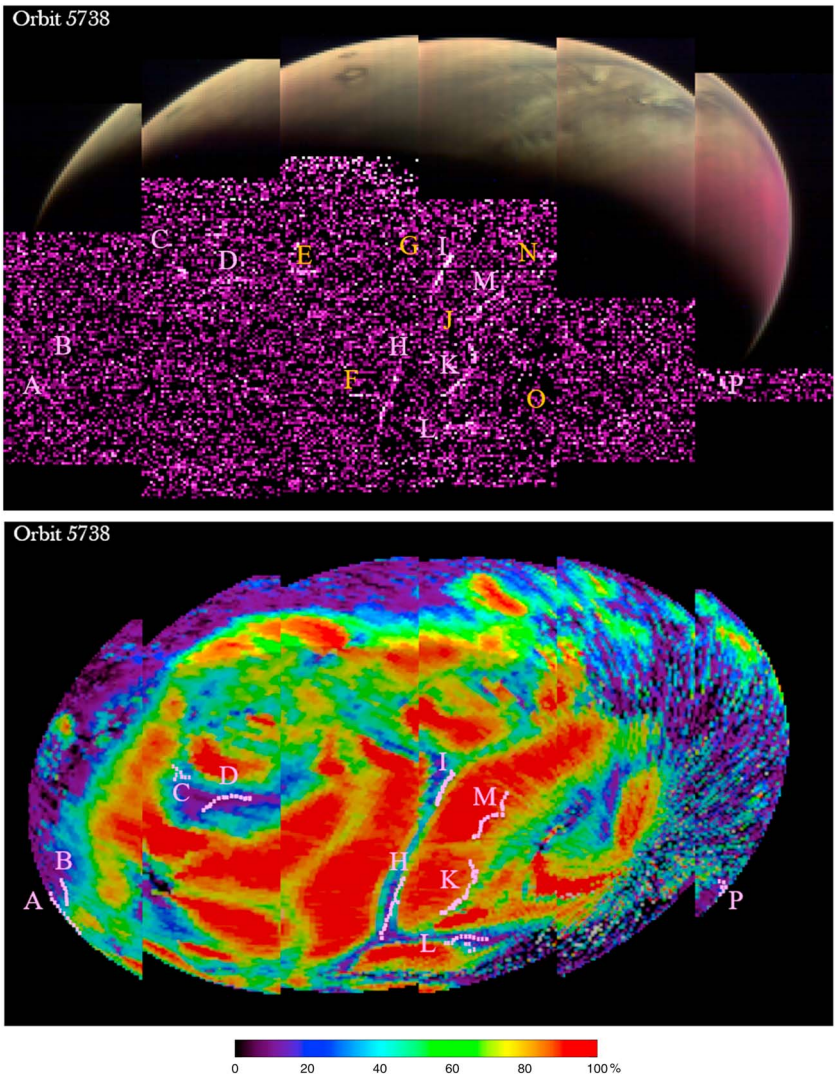


Figure 4. (top) Apoapse image of Mars from orbit 5738, preserving the six vertical swaths of the raw data format. The top portion shows the daylit side with middle UV colors mapped up to visible colors. North is to the left. The bottom portion of the data image shows the nightside imaged at high gain, using the same purple-white colorbar as Figure 1. The letters identify the locations of wisps and patches of emission analyzed in detail; the letters are shown in purple if spectral analysis confirms the auroral nature of the emission, and in orange if spectral analysis indicated an instrumental artifact. (bottom) The specific pixels in wisps and patches with confirmed auroral spectra are shown in purple with their identifying letter. Features identified as artifacts in the top panel are omitted from the bottom. The pixels are overplotted on Mars' crustal magnetic field topology from Brain et al. (2007) mapped into the observation coordinate system at the moment of each exposure. The red color indicates a high probability of closed magnetic field lines, and the dark blue color indicates a high probability of open field lines.

4. Conclusions

The opportunity to measure Mars' diffuse aurora at its strongest recorded levels strengthens the conclusion that the phenomenon must be global in scope. While the IUVS limb scans used in the discovery of diffuse aurora demonstrated that the phenomenon occurred wherever observations were obtained, the finite set of viewing geometries prevented a stronger conclusion about the spatial scale of the aurora. Images such as Figure 1 support the global nature, with relatively uniform emission around the limb and across the disk. Inlimb/outlimb measurements, sampling the region 90° away from the image limb, measured brightnesses comparable to the image limb. The image and limb scan brightnesses in Figure 3 approximately tracked each other, meaning that the global brightness varied approximately in phase around the planet.

The global nature of diffuse aurora is not surprising, given Mars' lack of a dynamo magnetic field, but these observations have provided the strongest evidence to date. We note that IUVS observations cannot prove that emission occurred on the small portion of nightside not visible to MAVEN, nor that aurora occurred on the dayside. The high energies of the particles and the weakness of crustal magnetic fields, however, make both likely. Ironically, the nightside aurora were so intense that IUVS could have detected the emission on the dayside if it did not occur so low in the atmosphere.

The combined auroral and energetic particle observations do not clearly distinguish between electron or proton precipitation as the cause. The particle fluxes, energies, and energy fluxes are comparable within about an order of magnitude, so neither can be ruled out based on ability to created bright aurora. Protons and electrons of sufficient energy can reach Mars' nightside: High-energy electrons are known to penetrate Mars' nightside to the observed altitudes in previous diffuse aurora observations when high-energy protons were absent (Schneider, Deighan, Jain, et al., 2015), and the large gyroradius for energetic protons means they too can reach Mars' nightside (Lillis et al., 2016; Luhmann et al., 2007). Further modeling work on particle trajectories, energy deposition, and emission physics is required to resolve the ambiguity, though efforts are hampered by the lack of relevant cross sections for electron and proton impact ionization and excitation at such high energies.

The event provided two new insights into the role of Mars crustal magnetic fields during space weather events. First, the imprint of crustal magnetic fields during Orbit 5738 shows they do play a role under certain circumstances. The data in hand, though, do not distinguish between two possible end-member sources of precipitating particles: low-energy electrons accelerated by field-aligned potentials, as for discrete aurora (Brain et al., 2006), or some type of crustal field control of the high-energy electrons responsible for the diffuse aurora. (Note that high-energy protons are not a likely source as gyroradii are larger than the observed features for energies above ~10 keV.) Further observation studies may glean either spectral or altitude information which could narrow down the possible energy range. Modeling of precipitation could give insights in the control of energetic electrons by crustal fields. Second, the lack of wisps and patches during the brightest aurora, when crustal fields were also present in the image frame, suggests that the dominant precipitating particles responsible for the aurora are not diverted or deflected to a significant degree. A future study will examine more closely whether small variations in emissions in other orbits with bright aurora might be associated with crustal magnetic fields. MAVEN's studies of space weather at Mars should improve after the upcoming solar minimum.

Acknowledgments
The MAVEN mission is supported by NASA in association with the University of Colorado and NASA's Goddard Space Flight Center. The authors thank Jean-Claude Gérard for useful discussions. The data may be obtained from the Planetary Atmospheres Node of the PDS using the filenames and version numbers in the text.

References

Bertaux, J.-L., Leblanc, F., Witasse, O., Quemerais, E., Lilensten, J., Stern, S. A., et al. (2005). Discovery of an aurora on Mars. *Nature*, *435*(7043), 790–794. https://doi.org/10.1038/nature03603

Brain, D. A., Halekas, J. S., Peticolas, L. M., Lin, R. P., Luhmann, J. G., Mitchell, D. L., et al. (2006). On the origin of aurorae on Mars. *Geophysical Research Letters*, *33*, L01201. https://doi.org/10.1029/2005GL024782

Brain, D. A., Lillis, R. J., Mitchell, D. L., Halekas, J. S., & Lin, R. P. (2007). Electron pitch angle distributions as indicators of magnetic field topology near Mars. *Journal of Geophysical Research*, *112*, A09201. https://doi.org/10.1029/2007JA012435

Deighan, J., Jain, S. K., Chaffin, M. S., Fang, X., Halekas, J. S., Clarke, J. T., et al. (2018). Discovery of a proton aurora at Mars. Nature Astronomy. https://doi.org/10.1038/s41550-018-0538-5

Gérard, J.-C., Soret, L., Libert, L., Lundin, R., Stiepen, A., Radioti, A., & Bertaux, J. L. (2015). Concurrent observations of ultraviolet aurora and energetic electron precipitation with Mars Express. *Journal of Geophysical Research*, *120*, 6749–6765. https://doi.org/10.1002/2015JA021150

Gérard, J. C., Soret, L., Shematovich, V. I., Bisikalo, D. V., & Bougher, S. W. (2017). The Mars diffuse aurora: A model of ultraviolet and visible emissions. *Icarus*, *288*, 284–294. https://doi.org/10.1016/j.icarus.2017.01.037

Halekas, J. S. (2017). Seasonal variability of the hydrogen exosphere of Mars. *Journal of Geophysical Research: Planets*, *122*, 901–911. https://doi.org/10.1002/2017JE005306

Jakosky, B., Lin, R. P., Grebowsky, J. M., Luhmann, J. G., Mitchell, D. F., Beutelschies, G., et al. (2014). The 2013 Mars Atmosphere and Volatile Evolution (MAVEN) mission to Mars. *Space Science Reviews*, *195*(1-4), 3–48. https://doi.org/10.1007/s11214-015-0139-x

Jakosky, B. M., Grebowsky, J. M., Luhmann, J. G., Connerney, J., Eparvier, F., Ergun, R., et al. (2015). MAVEN observations of the response of Mars to an interplanetary coronal mass ejection. *Science*, *350*(6261), aad0210. https://doi.org/10.1126/science.aad0210

Larson, D. E., Lillis, R. J., Lee, C. O., Dunn, P. A., Hatch, K., Robinson, M., et al. (2015). The MAVEN solar energetic particle investigation. *Space Science Reviews*, *195*(1-4), 153–172. https://doi.org/10.1007/s11214-015-0218-z

Lillis, R. J., Lee, C. O., Larson, D., Luhmann, J. G., Halekas, J. S., Connerney, J. E. P., & Jakosky, B. M. (2016). Shadowing and anisotropy of solar energetic ions at Mars measured by MAVEN during the March 2015 solar storm. *Journal of Geophysical Research: Space Physics*, *121*, 2818–2829. https://doi.org/10.1002/2015JA022327

Luhmann, J. G., Zeitlin, C., Turner, R., Brain, D. A., Delory, G., Lyon, J. G., & Boynton, W. (2007). Solar energetic particles in near-Mars space. *Journal of Geophysical Research*, *112*, E10001. https://doi.org/10.1029/2006JE002886

McClintock, W. E., Schneider, N. M., Holsclaw, G. M., Hoskins, A. C., Stewart, I., Deighan, J., et al. (2015). The Imaging Ultraviolet Spectrograph (IUVS) for the MAVEN mission. *Space Science Reviews*, *195*(1-4), 75–124. https://doi.org/10.1007/s11214-014-0098-7

Ritter, B., Gérard, J.-C., Hubert, B., Rodriguez, L., & Montmessin, F. (2018). Observations of the proton aurora on Mars with SPICAM on board Mars Express. *Geophysical Research Letters*, *45*, 612–619. https://doi.org/10.1002/2017GL076235

Schneider, N. M., Deighan, J. I., Jain, S. K., Stiepen, A., Stewart, A. I. F., Larson, D., et al. (2015). Discovery of diffuse aurora on Mars. *Science*, *350*(6261), aad0313. https://doi.org/10.1126/science.aad0313

Schneider, N. M., Deighan, J. I., Stewart, A. I. F., McClintock, W. E., Jain, S. K., Chaffin, M. S., et al. (2015). MAVEN IUVS observations of the aftermath of the Comet Siding Spring meteor shower on Mars. *Geophysical Research Letters*, *42*, 4755–4761. https://doi.org/10.1002/2015GL063863

Stevens, M. H., Evans, J. S., Schneider, N. M., Stewart, A. I. F., Deighan, J., Jain, S. K., et al. (2015). New observations of molecular nitrogen in the Martian upper atmosphere by IUVS on MAVEN. *Geophysical Research Letters*, *42*, 9050–9056. https://doi.org/10.1002/2015GL065319